Characteristics' relation model of asphalt pavement performance based on factor analysis

Tian, P, Shukla, A, Nei, L, Zhan, G & Liu, S

DOI 10.1016/j.ijprt.2017.07.007
ISSN 1996-6814
ESSN 1997-1400
Publisher: **Elsevier**

Available online at www.sciencedirect.com

ScienceDirect

International Journal of Pavement Research and Technology 11 (2018) 1–12

www.elsevier.com/locate/IJPRT

Characteristics' relation model of asphalt pavement performance based on factor analysis

Peng Tian [a,b], Ashish Shukla [c,*], Lei Nie [a,*], Gaofeng Zhan [a,d], Shuli Liu [c]

[a] College of Construction Engineering, Jilin University, Changchun 130026, China
[b] Network Information Center, Jilin Jianzhu University, Changchun 130118, China
[c] School of Energy, Construction and Environment, Faculty of Engineering, Environment and Computing, Coventry University, Coventry CV1 5FB, United Kingdom
[d] School of Transportation Science and Engineering, Jilin Jianzhu University, Changchun 130118, China

Received 24 December 2016; received in revised form 20 July 2017; accepted 24 July 2017
Available online 29 July 2017

Abstract

Pavement performance of asphalt is an important criterion for road engineering quality evaluation. Proposed research paper designed an orthogonal experiment using three asphalt mixtures, including SMA-13, AC-20 and ATB-25 to get their relation models and evaluate pavement performances. Totally twenty-seven samples from private companies have been selected and seven crucial parameters are analyzed via factor analysis. Further analysis concluded three main factors corresponding to the three main pavement performance parameters (i) high-temperature stability (ii) durability and (iii) shear resistance. Based on scores of each asphalt mixture's 3D scatter-map is plotted. Analysis found the relationship between three above-mentioned parameters. Relationship between the three main performance parameters has been established using graphical analysis. A separation plane can define the different types of asphalt mixtures' scatter distribution area, and get the regression equation for the plane. Based on the equation for the plane a more intuitionistic model has been made which describes the relationship of asphalt pavement performance.

Keywords: Road engineering; Asphalt; Index correlation; Surface fitting; 3D-model

1. Instruction

Globally produced 90% of asphalt (approx. 100 million tons) is used to construct the asphalt pavements [1,2]. Over 90% of roads and pavements are constructed from Asphalt in the Europe. It is a mixture of aggregates, which account for 91–97% of the total mix and a binder, commonly bitumen, which accounts of 3–9% of the total mix. Asphalt is not only used for construction of new road surfaces but also for maintenance and repair of roads [3]. Asphalt mixtures are the main construction materials of road engineering because of its road performance and durability. Researcher have found that pavement infrastructure plays an important role in the sustainability of urban systems [4,5], it can directly impact fuel consumption and vehicle emissions. This has been stated by researchers [5] that the pavement infrastructure is vital component of surface transportation. This has significant environmental impacts, making it important that pavement should exhibit high performance and durability. In the research of pavement performance, much attention has often been given to the life cycle assessment [4,6,7]; construction control [8,9,10]; gradation design [11,12,13,14] and physical and chemical

* Corresponding authors.
E-mail addresses: ashish.shukla@coventry.ac.uk, ashish.physik@gmail.com (A. Shukla).
Peer review under responsibility of Chinese Society of Pavement Engineering.

http://dx.doi.org/10.1016/j.ijprt.2017.07.007
1996-6814/

properties of asphalt and additive agents [15,16,17,18]. However, the comprehensive research on the relationship of pavement performance characteristics is few. Hou et al. [19] evaluated the pavement performance through model analysis using predicted dynamic modulus. Authors found that the Witczak models are useful in estimating pavement performance associated with the CAM model. Dai [20] developed a micromechanical finite-element (FE) model to predict dynamic modulus (E) and phase angle (d) of asphalt mixtures. D. Nazzal et al. [21] studied the long-term field performance and life cycle costs of the pavements. Authors found that Thermal and fatigue cracking were the main distresses that developed in the pavement sections. Ayar et al. [22] has investigated the healing capability of asphalt pavements. Author emphasized to conduct a more in-depth investigation of the contribution of healing capability to asphalt pavement design. Several experimental and modeling studies on pavement performance characteristics [23,24] have been reported. The pavement performance characteristics of asphalt mixture can be obtained by experiment but holistic pavement performance of asphalt mixture will not be possible. There will be no characteristics' model made for a comprehensive assessment. In the current research, a total of seven factors namely; (i) percentage of voids in aggregate (VV), (ii) percent voids in mineral aggregate (VMA), (iii) asphalt Saturation (VFA), (iv) Marshall Stability (MS), (v) Dynamic Stability (DS), (vi) Marshall residual stability ratio (MSR) (vii) and Freeze–thaw splitting strength ratio (TSR) have been assessed. In a total of twenty-seven samples of three asphalt mixtures SMA, ATB and AC have been used where SMA is stone mastic asphalt mixture, AC is asphalt concrete and ATB is asphalt treated base. ATB is a dense graded hot mix asphalt (HMA) having wide gradation band and lower asphalt content. In general ATB costs, less than typical HMA mixtures because the same can be produced with low cost aggregates and low percentage of asphalt binders.

With the factor analysis, one can explain roles of the seven different characteristics in pavement performance. This method provides the degree of characteristic with the factor score. Depending on the score, the relationships among characteristics have been established. Based on seven characteristics of three asphalt mixtures Factor analysis is also carried out. It has been found that three parameters namely high temperature stability, durability and shearing resistance plays major role in the pavement performance.

2. Materials and experiments

2.1. Theory of factor analysis

The quantitative analysis of the proposed research uses factor analysis and is partially based on the reasoning behind generating socio-geographical approach to scenarios analysis [25,26]. Factor analysis is a multivariate statistical analysis method, which studies the relationship between the sample correlation matrix and the number of variables or samples that have a certain relationship to the less than the number of no-observable factors (also known as the main factor). It has been widely used in many fields e.g. geology, economics, sociology, archeology, biology, medicine, and sports science [27,28,29].

2.2. Process of analysis

Fig. 1 shows process for analysis how factor analysis is carried out for the current study.

2.3. Data standardization

In order to avoid the difference of the data dimension, the experimental data have been standardized before the factor analysis using the Z-score as following equation:

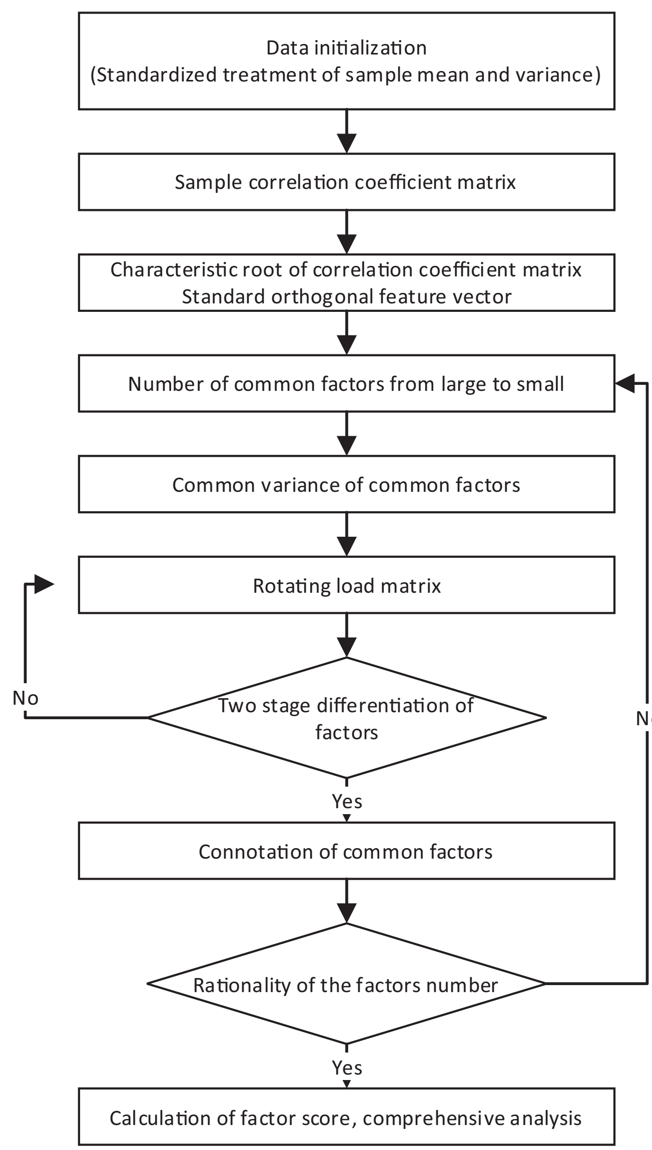

Fig. 1. Factor analysis procedure.

$$x^*_{ij} = \frac{x_{ij} - \overline{x}_j}{\sqrt{\frac{1}{n-1}\sum_{i=1}^{n}(x_{ij} - \overline{x}_j)^2}} \tag{1}$$

where $i = 1, 2, \cdots, n; j = 1, 2, \cdots p$, x_{ij} is the raw data, ($\overline{x}_j = \frac{1}{n}\sum_{i=1}^{n} x_{ij}$ is the average value of the j variable.

2.4. Mathematical model

The variables in use are listed in Table 1.

The numbers of variables are p, the sample size is n, where X is the data that have been standardized, such as the Eq. (2).

$$X = \begin{bmatrix} x_{11} & x_{12} & \cdots & x_{1p} \\ x_{21} & x_{22} & \cdots & x_{2p} \\ \cdots & \cdots & \cdots & \cdots \\ x_{n1} & x_{n2} & \cdots & x_{np} \end{bmatrix} \tag{2}$$

The average value of P ($x = (x_1, x_2, \cdots, x_p)$) is $\mu = (\mu_1, \mu_2, \cdots, \mu_p)$, the factor covariance matrix is $\Sigma = (\sigma_{ij})_{p\times p}$, the sample correlation coefficient matrix is $R = (\rho_{ij})_{p\times p}$. The general model of factor analysis can be determined as following:

$$\begin{cases} x_1 = \mu_1 + a_{11}f_1 + a_{12}f_2 + \cdots a_{1m}f_m + \varepsilon_1 \\ x_2 = \mu_2 + a_{21}f_1 + a_{22}f_2 + \cdots a_{2m}f_m + \varepsilon_2 \\ \cdots \\ x_p = \mu_p + a_{p1}f_1 + a_{p2}f_2 + \cdots a_{pm}f_m + \varepsilon_p \end{cases} \tag{3}$$

where $f_1, f_2, \cdots, f_m$ are common factors. ε_i is the special factor of $x_i (i = 1, 2, \cdots\cdots, p)$ and it is an non-measurable component of hidden variables. $a_{ij}(i = 1, 2, \cdots\cdots, p, j = 1, 2, \cdots\cdots, m)$ is the load of variable x_i in common factor f_i, It reflects the importance of the common factor to the variable, and has played an important role in the interpretation of common factors. We can simplify the Eq. (3) into matrix Eq. (4).

$$x = \mu + Af + \varepsilon \tag{4}$$

where $\mathrm{A} = (a_{ij})_{p\times m}$ is the factor load matrix. $f = (f_1, f_2, \cdots, f_m)\prime$ is the common factor vector, $\varepsilon = (\varepsilon_1, \varepsilon_2, \cdots, \varepsilon_p)'$ is the special factor vector [8].

Table 1
The variables in use.

Variables	Definition
X	The original data of samples.
R	The sample correlation coefficient matrix.
μ	The average value of x
$f_1, f_2, \cdots, f_m$	The common factors
ε_i	The special factor of x_i
$A = (a_{ij})_{p\times m}$	The factor load matrix
p	The numbers of variables.
n	The sample size.
$a_{ij}(i = 1, 2, \cdots\cdots, p, j = 1, 2, \cdots\cdots, m)$	The load of variable x_i in common factor f_i
$T_{m\times m}$	The orthogonal matrix
B	The rotation factor load matrix
V_j	The relative variance of the square of the elements of the j column

2.5. Factor rotation

The purpose of the establishment of the factor analysis model is to establish the relationship between the common factor and the real data. In that case, we need to study load of the various variables $x_1, x_2, \cdots, x_p$ in each factor. The column factor is easy to explain when the absolute value of the elements in a column is less and the gap is large. Therefore, when it is difficult to establish the relationship between the factors and the data, the factor rotation is also required. The absolute value of the elements in the factor load matrix is 0 or 1 of the polarization, which can be used to reduce the difficulty on relationship analysis. Kaiser, 1958 [30] proposed method namely maximum variance rotation (Varimax) has been used in this paper [30].

In the process of maximum variance rotation (factor rotation), set $T_{m\times m}$ as the orthogonal matrix, let $B = AT = (b_{ij})_{p\times m}$, $d_{ij}^2 = \frac{b_{ij}^2}{h_i^2}$, $\bar{d}_j = \frac{1}{p}\sum_{i=1}^{p} d_{ij}^2$, $V_j = \frac{1}{p}\sum_{i=1}^{p}(d_{ij}^2 - \bar{d}_j)^2$, $j = 1, 2, \cdots, m$ where B is the rotation factor load matrix, V_j is the relative variance of the square of the elements of the j column, it measures the difference between the square values of the elements of the j column. The method of maximum variance rotation is to find the orthogonal matrix T to reach the maximum of $V = V_1 + V_2 + \cdots V_m$.

2.6. Factor score

There are two common factor score calculation methods that have been used in the literature [31 namely (i) the weighted least square method and (ii) the regression method. In this paper, we use the regression method as expressed by the following [31]:

Let $y = x - \mu = (x_1 - \mu_1, x_2 - \mu_2, \cdots, x_p - \mu_p)' = (y_1, y_2, \cdots, y_p)'$, assume that $f = (f_1, f_2, \cdots, f_m)\prime$ is on the regression equation for y. It can be determined as the following:

$$\begin{cases} f_1 = \beta_{11}y_1 + \beta_{12}y_2 + \cdots + \beta_{1p}y_p \\ f_2 = \beta_{21}y_1 + \beta_{22}y_2 + \cdots + \beta_{2p}y_p \\ \cdots \\ f_m = \beta_{m1}y_1 + \beta_{m2}y_2 + \cdots + \beta_{mp}y_p \end{cases} \tag{5}$$

The matrix expression can be written as Eq. (6)

$$f = \beta y \tag{6}$$

where $\beta = (\beta_{ij})_{m\times p}$ and by the Eq. (7) as the following:

$$\begin{aligned} a_{ij} &= cov(x_i, f_j) \\ &= cov(x_i, \beta_{j1}y_1 + \beta_{j2}y_2 + \cdots + x_i, \beta_{jp}y_p) \\ &= \beta_{j1}cov(x_i, x_1) + \beta_{j2}cov(x_i, x_2) + \cdots \\ &\quad + \beta_{jp}cov(x_i, x_p) \\ &= \beta_{j1}\sigma_{i1} + \beta_{j2}\sigma_{i2} + \cdots + \beta_{jp}\sigma_{ip} \end{aligned} \tag{7}$$

Thus, A is:

$$A = \Sigma\beta' \tag{8}$$

where the β estimated value $\hat{\beta} = A\Sigma^{-1}$. When substituted into Eq. (6), we can get the estimate equation of factor score as following:

$$\hat{f} = \hat{\beta}y = A'\Sigma'(x - \mu) \tag{9}$$

We take $\bar{x}\hat{A}$ and S as estimate of μ, A and Σ. Then we put the observation data (x_i) of each sample into the Eq. (9) and get the corresponding factor score Eq. (10) as the following:

$$\hat{f}_i = \hat{A}'^{S^{-1}}(x_i - \bar{x}) \tag{10}$$

3. Laboratory experiments

3.1. Experiment scheme

According to Standard Test Methods of Bitumen and Bituminous Mixtures for Highway Engineering of China [32] experiments used three kinds of asphalt mixtures with different gradation characteristics as the experimental materials namely ATB, AC and SMA, where ATB is, a dense graded asphalt stabilized macadam, AC is a dense graded asphalt concrete and SMA is the stone mastic asphalt. According to the orthogonal experimental method [33], design experiment scheme should match the three characteristics of asphalt mixture. With the aperture of 4.75 mm diameter as the cut-off point of the coarse and fine aggregate, three sets of coarse aggregate ratio curves and three sets of fine aggregate ratio curves are listed in Table 2.

The three levels of coarse aggregate and fine aggregate are the three curve positions of grading curve in Standard Test Methods of Bitumen and Bituminous Mixtures for Highway Engineering of China [32]. There are upper line and lower line in the standard curve. In this paper, the middle-curve is the median line of grading curve range. The up-curve is the bisector between the upper line and median one of it. The down-curve is the bisector between the lower line and median one of it. The three levels of the asphalt aggregate ratio are 6.3%, 6.4% and 6.5%. The grading scheme is shown in Table 2.

Asphalt mixture specimen is produced on the standard compaction method. The specimen's sizes and the corresponding experiments are listed in Table 3.

According to the experimental arrangement in Table 3, in accordance with the relevant standard procedure [32], the experiment result is shown in Table 4.

Table 2
Grading scheme.

Plan	31.50	26.50	19.00	16.00	13.20	9.50	4.75	2.36	1.18	0.60	0.30	0.15	0.08
ATB1	100.00	93.62	67.93	59.79	51.31	41.78	29.70	23.02	18.62	14.28	11.06	7.90	3.06
ATB2	100.00	93.79	67.95	59.79	51.33	41.63	29.85	26.26	21.32	16.51	13.01	9.31	3.61
ATB3	100.00	93.65	67.82	59.72	51.14	41.48	30.42	19.17	15.01	11.40	8.77	6.17	2.15
ATB4	100.00	94.65	72.26	64.81	56.13	45.94	29.58	23.49	18.89	14.50	11.21	8.09	3.09
ATB5	100.00	94.59	72.53	65.32	56.71	46.76	30.38	26.56	21.67	16.80	13.28	9.44	3.66
ATB6	100.00	94.62	72.62	65.32	56.75	46.84	30.41	18.66	14.62	11.14	8.85	6.22	2.47
ATB7	100.00	92.94	63.89	55.05	46.49	37.42	30.35	22.64	18.36	14.01	10.93	7.72	3.02
ATB8	100.00	92.87	63.52	54.83	46.26	37.33	30.15	26.66	21.82	16.97	13.36	9.62	3.90
ATB9	100.00	92.82	63.88	55.18	46.44	37.45	30.33	18.77	14.64	11.15	8.67	6.20	2.23
AC1	100.00	100.00	92.59	85.41	74.39	58.70	41.10	28.79	22.61	17.49	12.30	8.20	4.59
AC2	100.00	100.00	92.59	84.99	73.31	56.60	41.30	31.91	27.31	21.91	15.11	9.70	5.10
AC3	100.00	100.00	92.51	85.40	74.39	58.81	40.60	24.80	16.39	11.71	8.59	6.21	3.80
AC4	100.00	100.00	94.79	88.30	78.20	63.81	41.30	28.11	22.00	16.99	11.99	8.11	4.49
AC5	100.00	100.00	95.31	88.61	78.10	63.10	41.59	31.69	27.60	22.31	15.39	9.89	5.31
AC6	100.00	100.00	95.20	89.89	78.99	64.89	40.71	24.41	16.39	11.81	8.60	6.19	3.71
AC7	100.00	100.00	89.89	82.00	69.99	52.99	41.29	29.01	21.91	16.71	11.91	8.11	4.59
AC8	100.00	100.00	89.91	81.60	69.09	51.29	41.40	32.10	26.79	21.41	15.01	9.89	5.39
AC9	100.00	100.00	89.90	82.20	70.69	54.40	41.01	25.40	16.39	11.49	8.49	6.21	3.81
SMA1	100.00	100.00	100.00	100.00	86.37	64.42	27.00	20.58	18.08	15.90	14.36	12.77	8.50
SMA2	100.00	100.00	100.00	100.00	86.37	64.41	27.00	23.23	20.54	17.96	16.12	14.22	9.33
SMA3	100.00	100.00	100.00	100.00	86.41	64.46	27.03	18.02	15.82	14.14	13.00	11.81	8.15
SMA4	100.00	100.00	100.00	100.00	88.85	70.85	26.99	20.58	18.08	15.90	14.36	12.77	8.50
SMA5	100.00	100.00	100.00	100.00	88.85	70.85	27.00	23.23	20.54	17.96	16.12	14.22	9.33
SMA6	100.00	100.00	100.00	100.00	88.89	70.89	27.03	18.02	15.82	14.14	13.00	11.81	8.15
SMA7	100.00	100.00	100.00	100.00	83.89	57.98	26.99	20.58	18.08	15.90	14.36	12.77	8.50
SMA8	100.00	100.00	100.00	100.00	83.89	57.98	27.00	23.23	20.54	17.96	16.12	14.22	9.33
SMA9	100.00	100.00	100.00	100.00	83.93	58.03	27.03	18.02	15.82	14.14	13.00	11.81	8.15

Table 3
Specimen for Experiment.

Size	Manufacture method	Experiment project
ϕ101.6 mm × 63.5 mm Cylindrical specimens	Marshall Compaction Method	Mixture density experiment Marshall stability experiment Immersion Marshall experiment Splitting experiment Freeze-thaw splitting experiment
300 mm × 300 mm × 50 mm Prism specimen	Rolling Wheel Method	Wheel tracking test

Table 4
The experiment result.

Plan	VV (%)	VMA (%)	VFA (%)	MS(KN)	DS(times/mm)	MSR (%)	TSR (%)
ATB1	3.77	12.00	68.60	11.40	1908.00	81.33	78.31
ATB2	3.76	12.20	69.10	11.90	1349.00	83.42	86.31
ATB3	4.27	12.60	66.10	10.10	1536.00	86.54	84.52
ATB4	3.98	12.40	67.90	11.00	2297.00	86.00	77.61
ATB5	4.27	12.70	66.40	12.20	1852.00	82.90	84.01
ATB6	5.41	13.70	60.50	9.60	2345.00	83.91	85.41
ATB7	3.74	12.10	69.00	11.20	1812.00	80.15	74.10
ATB8	3.73	12.50	70.10	11.10	1468.00	97.32	64.51
ATB9	5.03	13.30	62.20	10.00	1653.00	81.63	85.31
AC1	4.60	14.50	68.28	11.90	7873.00	98.20	97.98
AC2	4.10	14.20	71.13	12.20	3499.00	86.80	92.06
AC3	7.30	19.70	62.94	8.00	3936.00	87.10	73.16
AC4	4.30	15.50	72.26	8.60	7002.00	87.40	90.17
AC5	4.70	14.60	67.81	13.30	6300.00	87.20	99.36
AC6	7.80	17.40	55.17	8.10	3001.00	91.90	98.59
AC7	3.50	13.60	74.26	11.60	7000.00	99.30	98.98
AC8	4.10	13.20	68.94	14.00	2623.00	87.30	96.96
AC9	7.60	17.20	55.81	8.50	7874.00	91.70	95.40
SMA1	4.91	18.75	73.89	6.40	9000.00	94.43	94.99
SMA2	3.76	17.77	78.89	6.11	10500.00	91.25	87.76
SMA3	4.95	18.79	73.69	5.61	5250.00	88.23	99.89
SMA4	3.78	17.69	78.73	5.94	7000.00	95.79	96.61
SMA5	3.17	17.17	82.10	4.76	5727.27	71.19	71.19
SMA6	4.81	18.57	74.17	5.19	2739.13	74.80	82.47
SMA7	4.50	18.46	76.22	5.08	9000.00	74.02	80.78
SMA8	2.50	16.75	85.16	5.97	5250.00	76.71	82.65
SMA9	4.62	18.56	75.36	5.86	4846.16	81.15	99.49

In Table 4, the first column VV (%) is the percentage of voids in aggregate. The value of AC3, AC6 and AC9 is relatively high. The value of rest is relatively average. VMA (%) is the percent voids in mineral aggregate. The value of AC3, AC6 and AC9 is close to the value of SMA materials. The VMA of rest AC materials are close to the value of ATB materials. VFA (%) is the asphalt saturation. The value of AC and ATB materials are between 55% and 74%, but VFA value of SMA materials are above 74%. MS is the Marshall stability. The value of SMA materials is obviously lower than that of AC and ATB materials. And the performance of ATB materials is more stable than that of the others. The Dynamic stability (DS) values of ATB materials are lower than those of the others. The fluctuation of DS in AC and SMA is great. MSR is the Marshall residual stability ratio. TSR is the freeze–thaw splitting strength ratio. There are no significant differences in MSR and TSR. That means the levels of ATB, AC and SMA materials are similar to each other for the index of MSR and TSR.

3.2. Factor loadings

The number of factors is obtained by trial from large to small and is starting from 4. However, no solutions have been found for factor contribution rate 4. Then try to number 3, and get the solution on contribution rate 3. During the calculation, the maximum variance rotation method is used to carry on the factor rotation. The factor loading results are shown in Table 5.

Where VV is the percentage of voids in aggregate, VMA is the percent voids in mineral aggregate, VFA is asphalt saturation, MS is Marshall Stability, DS is dynamic stability, MSR is the Marshall residual stability ratio, TSR is the

Table 5
Factor contribution rate.

Characteristics	Contribution rate (%)		
	1	2	3
Percentage of voids in aggregate (VV)	7.1958	89.8003	2.6178
Percent voids in mineral aggregate (VMA)	95.8148	1.0733	2.6804
Asphalt saturation (VFA)	15.1233	84.3046	0.1713
Marshall stability (MS)	82.7146	0.7883	2.8918
Dynamic stability (DS)	25.2736	2.8457	20.4020
Marshall residual stability ratio (MSR)	2.4160	1.1692	47.6516
Freeze-thaw splitting strength ratio (TSR)	2.5145	0.8682	47.5613
Total contribution rate of each factor	33.0075	25.8357	17.7109

Table 6
The maximum likelihood estimate of specific variance.

VV	VMA	VFA	MS	DS	MSR	TSR
0.005	0.005	0.005	0.136	0.515	0.488	0.491

Table 7
Scores of factors.

Plan	High-temperature stability	Shear resistance	Durability
AC 1	−0.7839	−0.1000	2.1534
AC 2	−0.6354	−0.3525	0.7718
AC 3	1.4218	1.8223	−0.3176
AC 4	−0.0629	−0.2762	0.3845
AC 5	−0.6972	0.0358	1.6724
AC 6	0.3572	2.4352	0.4962
AC 7	−0.9873	−1.0077	2.1697
AC 8	−1.1084	−0.2653	1.1642
AC 9	0.2335	2.2527	0.8887
ATB 1	−1.1699	−0.1345	−1.1301
ATB 2	−1.1945	−0.2472	−0.4742
ATB 3	−1.0420	0.2326	−0.8492
ATB 4	−1.0807	−0.0197	−0.8629
ATB 5	−1.0701	0.1732	−0.5055
ATB 6	−0.7210	1.1546	−1.0365
ATB 7	−1.0787	−0.1360	−1.4431
ATB 8	−1.0377	−0.3037	−0.6466
ATB 9	−0.8159	0.8833	−1.1813
SMA 1	0.9729	−0.1749	1.3117
SMA 2	0.7815	−0.9704	0.7642
SMA 3	1.1039	−0.0478	0.5342
SMA 4	0.7010	−0.9900	1.0922
SMA 5	1.1010	−1.1011	−2.2193
SMA 6	1.3616	0.1087	−1.6125
SMA 7	1.2953	−0.2326	−1.0926
SMA 8	0.7976	−1.7502	−1.0310
SMA 9	1.1213	−0.2537	0.0584

freeze–thaw splitting strength ratio. In Table 2, it can be seen that, the contribution of each factors is 33.01%, 25.84% and 17.71%, the cumulative contribution rate is 76.55%. That means the three factors reflect the pavement performance characteristics of asphalt mixture.

In Table 5, MS and VMA have larger factor loadings in the first common factor. In a certain extent, it is match with the Marshall Stability and mixture gradation relationship theory, "No matter what level the coarse aggregate structure is, the fine aggregate structure has a significant influence on the stability of asphalt mixture Marshall" [34,35]. That is to say, the first common factor reflects the high temperature stability of asphalt mixture. In the second common factor variables, VV and VFA have greater loading values, and have inverse relation between them. With the increase in VV, the asphalt saturation decreased, the water absorption rate increased, and the mechanical properties (modulus, splitting strength and shear strength) of the asphalt mixture decreased [36]. The second factor can be defined as asphalt mixture shear resistance factor. In the column of third common factor, the contribution rate of DS, MSR and TSR is ten to twenty times to the other indicators. That reflects the durability of asphalt mixture [37,38,39]. Thus, the third common factor can be defined as the durability factor.

3.3. The maximum likelihood estimate of specific variance

The maximum likelihood estimate of the special variance has been obtained using the principal factor method as shown in Table 6.

When the special variance is greater or equal to 1, there will be Heywood Phenomenon. That means there are problems in the factor analysis and the number of factors is not applicable to this model. [40] The special variance estimation value in Table 6 shows that, each variable has smaller special variance, there is no Heywood Phenomenon. That indicates the model with three-factors has a good fitting effect.

3.4. The factor scores

According to the three factor model, the factor scores were calculated, and formed into matrix. The scores are shown in Table 7.

4. Characteristics' distribution model of pavement performance

4.1. Scatter diagram of factor scores

The three factors are used as the three axes to establish three-dimensional space. According to the factor score, the scattered points are drawn in the three-dimensional space. In the Fig. 2, based on the performance characteristics of the road (three axes), the three kinds of asphalt mixture pavement performance factor score in the three-dimensional graphics form three relatively independent scattered point distribution groups. These three distribution groups reflect a distinct, unique way with performance characteristics. It is closely related to the performance of the road, the composition of the mixture, the performance of the mixture, and the related indexes are closely related, and different gradation characteristics and physical properties show different road performance characteristics.

In order to facilitate observation and analysis, the three-dimensional scattered point distribution map from the three-axial direction, as shown in Figs. 3–5.

4.2. Partition plane for distributed region

The factor scores of three kinds of pavement performance can be clearly divided by the partition plane. The intersection points of the different asphalt pavement performances are represented by the intersection of the divisional plane and axes.

The dividing plane is shown in Fig. 6. That shows the scattered points of AC, ATB and SMA characteristic are gathered in own regions. The fitting equation of the dividing plane is the formula (Eq. 11), (Eq. 12). The X-axis represents the high temperature stability, the Y-axis represents the shear resistance, and the Z-axis represents the durability.

$$1.4x + z + 1 = 0 \tag{11}$$

$$1.3x - y - 0.8 = 0 \tag{12}$$

The factor score distribution area can be completely separated by two orthogonal partition planes, which means that the different mix ratios of asphalt mixture can be distinguished by factor analysis. At the same time, the plane equation of two orthogonal split planes can be established, which shows the proportional relationship in the various performances' indexes.

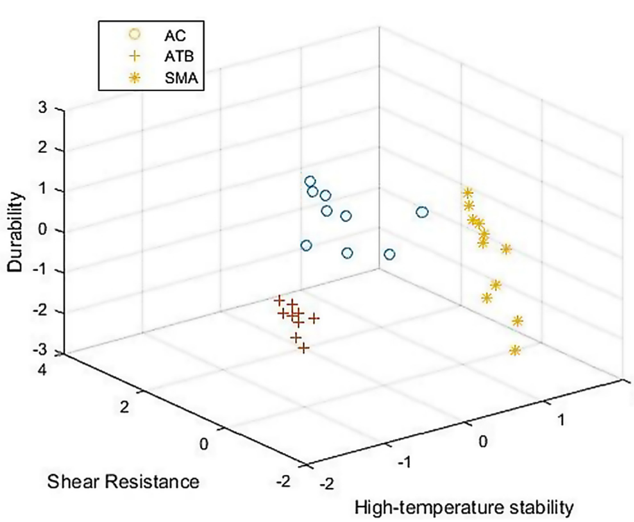

Fig. 2. Factor score 3D scatter diagram.

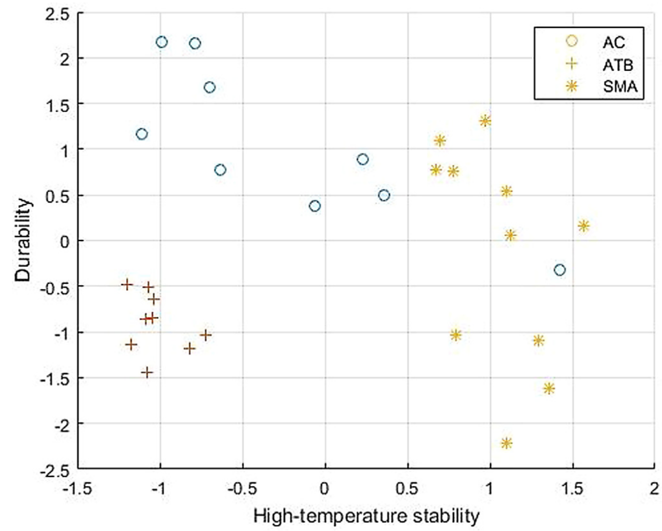

Fig. 3. Durability and high temperature stability factor score.

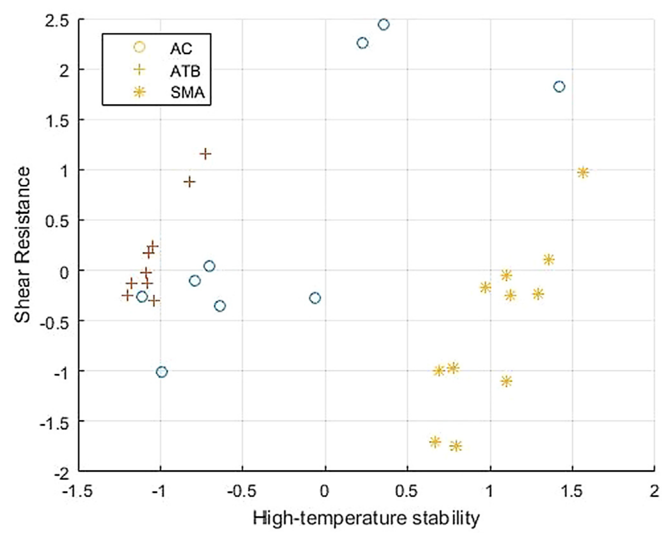

Fig. 4. Shear resistance and high temperature stability factor score.

4.3. Characteristic index analysis

Fig. 6 and Eq. (11) show that the dividing plane-1 is parallel to the axis Y, and splitting the factor score of ATB from other two asphalt mixtures. That reflects ATB asphalt performance is different from other two kinds of asphalt mixtures in durability and high temperature stability. But there is no significant difference in shear resistance. The characteristics of the ATB asphalt mixture can be observed clearly in Fig. 3. At the same time, it can be seen that the AC asphalt mixture is more prominent in the durability, while the SMA asphalt mixture shows more superior performance of high temperature stability. ATB asphalt mixture is not outstanding in high temperature stability and durability.

Fig. 6 and Eq. (12) show that the split plane-2 is parallel to the axis Z, and splitting the factor score of SMA from

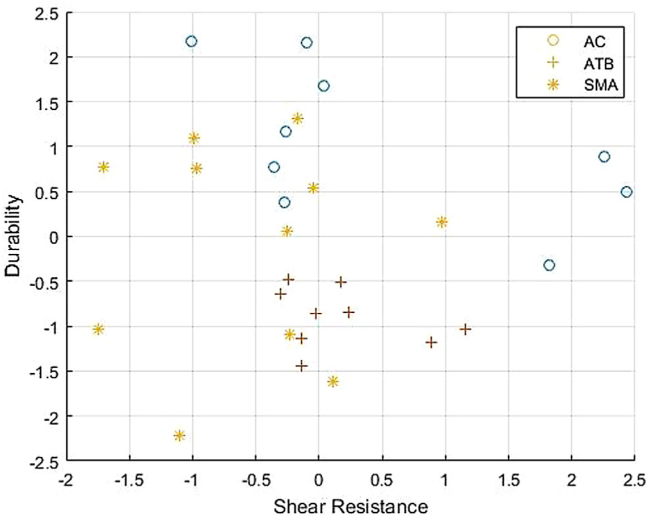

Fig. 5. Shear resistance and durability factor score.

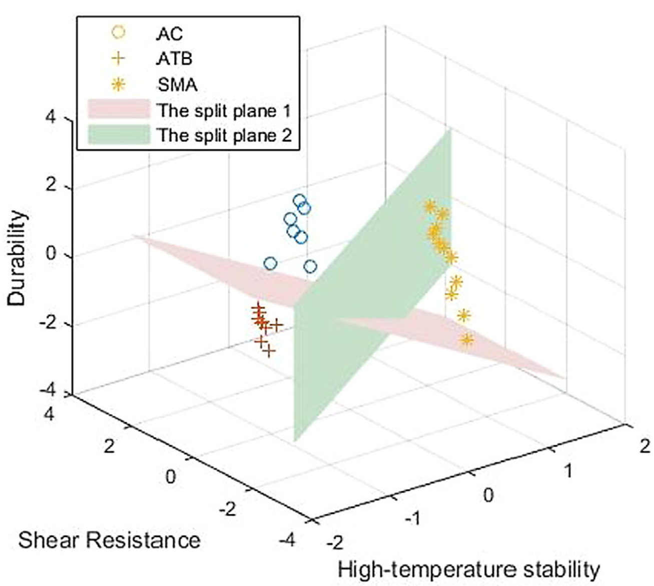

Fig. 6. Factor score three dimensional scattered point region.

other two. That reflects SMA asphalt performance is different from other two in high temperature stability and share resistance. But there is no significant difference in durability. It can be seen clearly in Fig. 4. At the same time, SMA showed excellent high temperature stability, but the shear resistance of ATB asphalt mixture, AC seems to have a good performance in the shear resistance and high temperature stability, but the overall distribution is more dispersed, the performance is not stable and not prominent.

In Fig. 5, the characteristics of the asphalt mixture are not significant, and the distribution of the sample points is relatively dispersed, and there are no significant distribution characteristics. That shows the relationship of shear resistance and durability is not obvious.

5. Factor score distribution surface fitting

5.1. Green spline interpolation of the factor score

Because of the limited number of samples, the simplicity of the surface fitting can produce large errors, which is not conducive to building data model and surface fitting, as shown in Fig. 7. Therefore, in order to improve the data density, the approximate distribution of the finite scattered point data is estimated by the interpolation method.

In this paper, we use the interpolation algorithm of the three-dimensional double harmonic Green function. The interpolation surface is a linear combination of the Green's function in the center of the sample distribution. By adjusting the weight of each point to optimize the surface to achieve the purpose of the distribution points through the sample [41,42]. The performance factor score 3D interpolation surfaces of AC, ATB and SMA are shown in Figs. 8–10.

5.2. Fitting of the factor score interpolation surface

By the method of least squares, the ATB, SMA and AC asphalt pavement performance factor scores interpolation

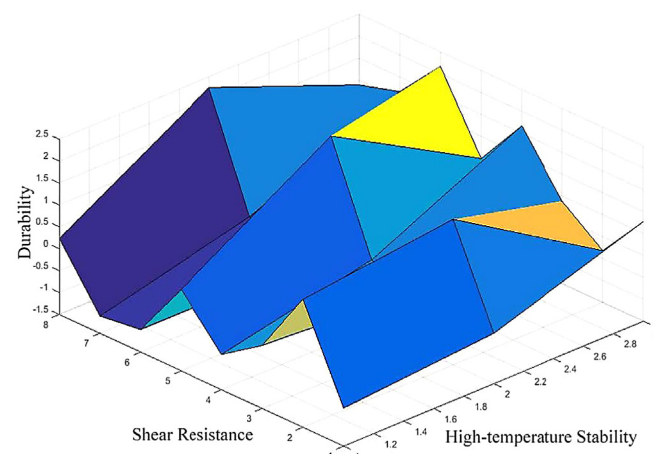

Fig. 7. Factor score surface of asphalt pavement performance.

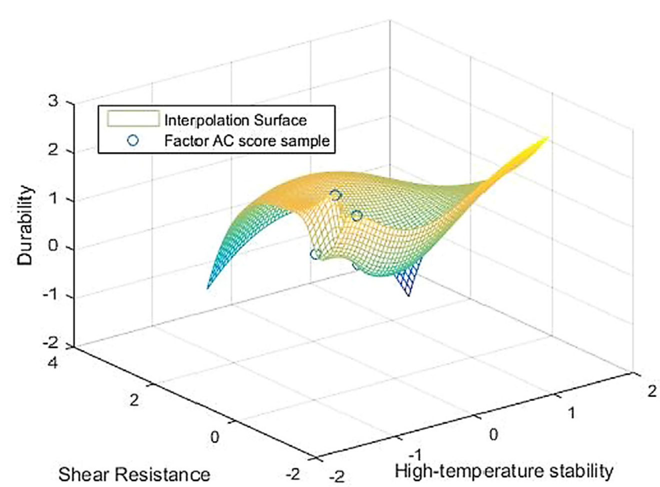

Fig. 8. AC factor score interpolation surface.

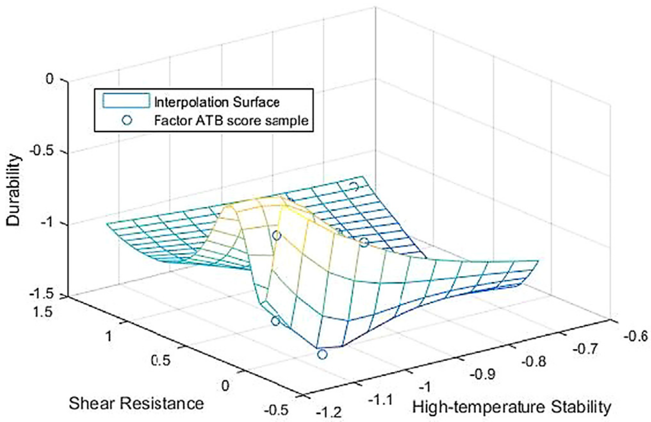

Fig. 9. ATB factor score interpolation surface.

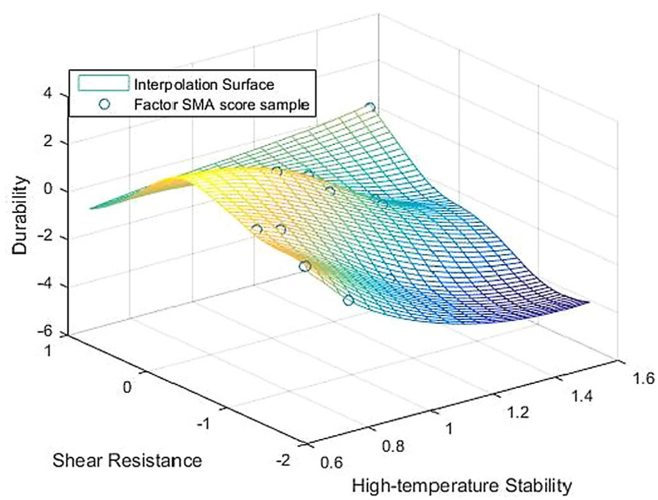

Fig. 10. SMA factor score interpolation surface.

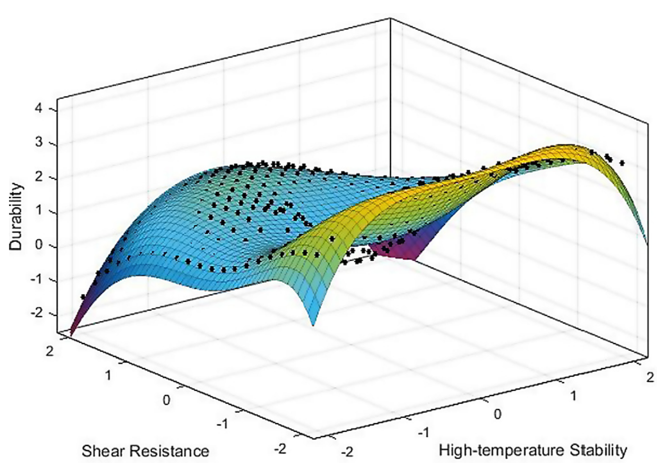

Fig. 11. Fitting surface of AC factor score.

surface is fitted. The coefficients of N polynomials are calculated and the expressions of the fitting surfaces are arranged.

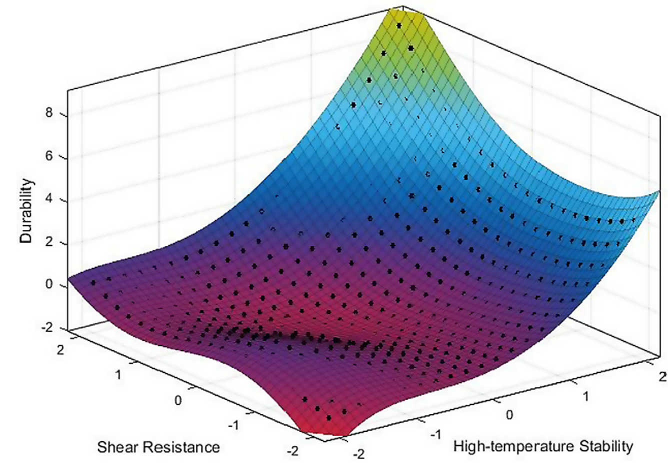

Fig. 12. Fitting surface of ATB factor score.

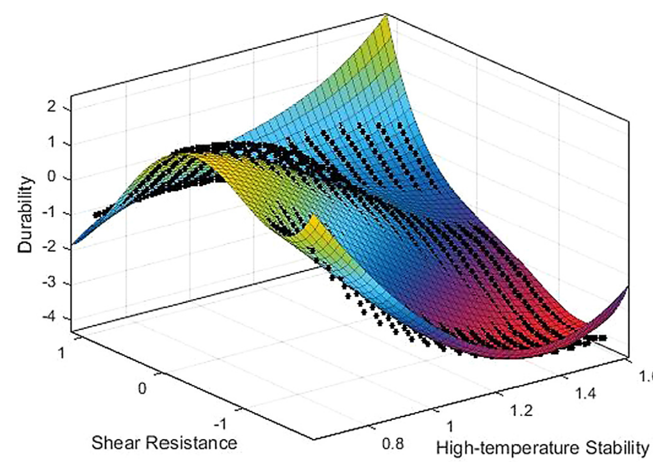

Fig. 13. Fitting surface of SMA factor score.

The fitting surface of AC asphalt mixture is shown in Fig. 11, and the fitting equation is shown in Eq. (13).

$$\begin{aligned} f(x,y) = {} & 0.884 - 0.029x + 0.415y + 0.465x^2 \\ & - 0.291xy + 0.803y^2 + 0.046x^3 - 0.36x^2y \\ & - 0.077xy^2 - 0.5y^3 - 0.096x^4 + 0.014x^3y \\ & - 0.168x^2y^2 + 0.047xy^3 - 0.092y^4 \\ & + 0.027x^4y - 0.007x^3y^2 + 0.036x^2y^3 \\ & + 0.014xy^4 + 0.058y^5 \end{aligned} \tag{13}$$

The fitting surface of ATB asphalt mixture is shown in Fig. 12, and the fitting equation is shown in Eq. (14).

$$\begin{aligned} f(x,y) = {} & -1.325 + 0.213x - 0.274y + 0.951x^2 \\ & + 0.553xy + 0.374y^2 + 0.135x^3 + 0.072x^2y \\ & + 0.283xy^2 + 0.283y^3 - 0.051x^4 - 0.044x^3y \\ & - 0.029x^2y^2 - 0.061xy^3 + 0.005y^4 + 0.014x^5 \\ & + 0.007x^4y - 0.01x^3y^2 - 0.008x^2y^3 \\ & - 0.009xy^4 - 0.023y^5 \end{aligned} \tag{14}$$

Table 8
List of fitting effect evaluation parameter.

Surface-fit	Variance	Standard deviation	Determination coefficient	Adjusted determination coefficient
Score-AC	10.26	0.1561	0.9804	0.9795
Score-ATB	4.06	0.0983	0.9972	0.9971
Score-SMA	25.93	0.1572	0.9906	0.9905

Table 9
Verification data.

Plan	VV	VMA	VFA	MS	DS	MSR	TSR
AC-c	4.0	13	70.5	16.9	4211	94.7	85.8
ATB-c	4.0	13	69.2	12.3	2104	96.1	80.7
SMA-c	3.6	17.2	78.9	10.6	6101	89.2	81.2

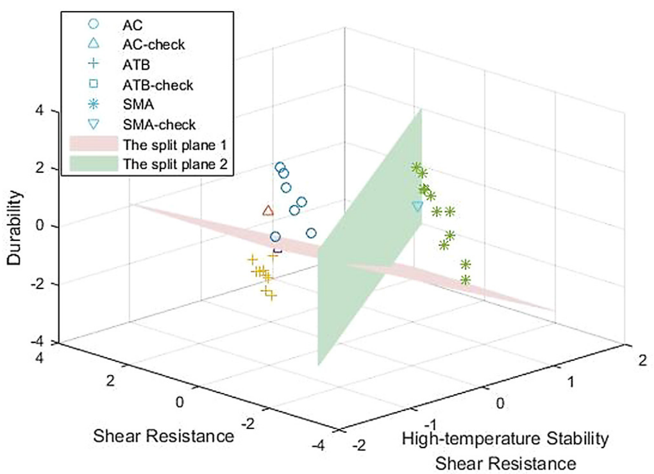

Fig. 14. Partition surface of factor score.

The fitting surface of SMA asphalt mixture is shown in Fig. 13, and the fitting equation is shown in Eq. (15).

$$f(x,y) = -4.371 + 22.17x - 7.254y \pm 23.95x^2 + 11.48xy - 1.39y^2 + 6.83x^3 - 6.33x^2y - 3.484xy^2 + 0.23y^3 + 1.554x^3y + 2.794x^2y^2 + 0.536xy^3 + 0.7y^4 \quad (15)$$

In statistics, the model's fitting degree is usually measured by the variance, the adjusted determination coefficient, and the standard deviation. That is shown in Table 8.

The smaller the variance and the standard deviation, the better the surface fitting effect; the determination coefficient and the adjusted determination coefficient are close to 1, the fitting effect is better. It can be seen from Table 5 that the factor score surface fitting effect of AC, ATB and SMA asphalt pavement performance is good and reaches the high level of fitting effect evaluation. The fitting surface accurately represents the distribution of the factor score in a three factor space.

6. Verification analysis

The experimental data of the construction site laboratory are collected in the same project in Table 9, taking them as the experimental verification data, repeat the steps of the analysis.

After the factor analysis, the factor scores of verification data are plotted in the scatter diagram as shown in Fig. 14. The discrete points of the verification samples are distributed in the region of different asphalts mixtures, and meet the regional division of the original partition surface. That shows the distribution of different sets of features can be effectively used for the distribution of asphalt pavement performance.

7. Conclusions

Based on the factor analysis, the seven pavement performance indexes are reduced to three factors, which symbolize high temperature stability, durability and shearing resistance respectively. That laid the foundation for the analysis of the performance characteristics of asphalt mixture with different gradation. Following conclusions have been made from the current research:

(1) Based on the three scores of pavement performance for each sample, a 3D scattered point distribution chart was drawn. The performance of three asphalt mixtures showed distinct characteristics. There three scattered point distribution groups, independent of each other. That can be used to distinguish the pavement performance characteristics of asphalt mixture.
(2) The split plane can be mapped on the 3D scattered point distribution chart and can be used to segment the area of three scattered point distribution groups. On the basis of fitting method, the formula of split plane can be developed, and the initial model of relationship in pavement performance indexes can be established. The factor score of the validation data is consistent with the model, which proves the model is valid. Unlike other studies, we visualize the results of the factor analysis. The distribution of scattered points is classified and the distribution space is fitted. They are taken as the characteristics' relation models. It is not a factor score, or a description, but the overall distribution to describe the pavement performance. With the deepening of the research, it may develop into four dimensions, five dimensions and so on.
(3) Based on the number of characteristics and samples, the experimental data can only reflect the pavement performance of an asphalt mixture on a certain level.

It is difficult to attain a higher accuracy of either the regional distribution map, or the pavement performance equation. If a larger data base were to be used in the factor analysis, a higher level of data and knowledge would be achieved. Through the long-term accumulation of data, both the data model of pavement performance relationship and the accuracy of model fitting will be gradually improved.

(4) Different material compositions determine the different asphalt pavement performances, and different pavement performance indexes reflect the different characteristics of an asphalt mixture. By the method of factor analysis, the corresponding relationship between pavement performance and the composition of asphalt mixture can be discovered and emphasized.

References

[1] A. Jamshidi, M.O. Hamzah, K. Kurumisawa, T. Nawa, B. Samali, Evaluation of sustainable technologies that upgrade the binder performance grade in asphalt pavement construction, Mater. Des. 95 (2016) 9–20.

[2] M.G. Mothe, L.F.M. Leite, C.G. Mothe, Kinetic parameters of different asphalt binders by thermal analysis, J. Therm. Anal. Calorim. 106 (2011) 679–684.

[3] L.M. McCarthy, J.M. Gudimettla, G.L. Crawford, M.C. Guercio, D. Allen, Impacts of variability in coefficient of thermal expansion on predicted concrete pavement performance, Construct. Build. Mater. 93 (2015) 711–719.

[4] J. Harvey, J. Meijer, Kendall Life Cycle Assessment of Pavements. Highlight of FHWA-HIF-15-001. Department of Transportation, FHWA. U.S. (2014).

[5] P. Inyim, J. Pereyra, M. Bienvenu, A. Mostafavi, Environmental assessment of pavement infrastructure: A systematic review, J. Environ. Manage. 176 (2016) 128–138.

[6] J. Lidicker, N. Sathaye, S. Madanat, A. Horvath, Pavement resurfacing policy for minimization of life-cycle costs and greenhouse gas emissions, J. Infrastruct. Syst 19 (2) (2013) 129–137.

[7] W.H. Roudebush, Environmental Value Engineering (EVE) Environmental Life Cycle Assessment of Concrete and Asphalt Highway Pavement Systems. Highlights of PCA R&D Serial No. 2088. Portland Cement Association, Illinois, (1996).

[8] Q. Xu, G.K. Chang, Adaptive quality control and acceptance of pavement material density for intelligent road construction, Automation Construct. 62 (2016) 78–88.

[9] Q. Xu, J.A. Prozzi, A time-domain finite element method for dynamic viscoelastic solution of layered half-space responses under loading pulses, Comput. Struct. 160 (2015) 20–39.

[10] R.D. Horan, G.K. Chang, Q. Xu, V.L. Gallivan, Improving quality control of hot mix asphalt paving using intelligent compaction technology, Transp. Res. Rec. 2268 (2012) 82–91.

[11] M. Pettinari, A. Simone, Effect of crumb rubber gradation on a rubberized cold recycled mixture for road pavements, Materials Des. 85 (2015) 598–606.

[12] A. Golalipour, E. Jamshidi, Y. Niazi, Z. Afsharikia, M. Khadem, Effect of Aggregate Gradation on Rutting of Asphalt Pavements, Proc. Soc. Behav. Sci. 53 (3) (2012) 440–449.

[13] K. Vislavičius, H. Sivilevičius, Effect of reclaimed asphalt pavement gradation variation on the homogeneity of recycled hot-mix asphalt, Arch. Civil Mech. Eng. 13 (3) (2013) 345–353.

[14] Q. Guo, Y. Bian, L. Li, Y. Jiao, J. Tao, Chengxiu Xiang Stereological estimation of aggregate gradation using digital image of asphalt mixture, Construct. Build. Mater. 94 (30) (2015) 458–466.

[15] S.H. Yang, Li-C. Lee, Characterizing the chemical and rheological properties of severely aged reclaimed asphalt pavement materials with high recycling rate, Construct. Build. Mater. 111 (2016) 139–146.

[16] P. Cong, Y. Zhang, N. Liu, Investigation of the properties of asphalt mixtures incorporating reclaimed SBS modified asphalt pavement, Construct. Build. Mater. 113 (2016) 334–340.

[17] M.E. Abdullah, K.A. Zamhari, M.R. Hainin, E.A. Oluwasola, N.A. Hassan, Nur Izzi Md. Yusoff, Engineering properties of asphalt binders containing nanoclay and chemical warm-mix asphalt additives, Construct. Build. Mater. 112 (2016) 232–240.

[18] A. Vaitkus, D.s Čygas, A. Laurinavičius, V. Vorobjovas, Z. Perveneckas, Influence of warm mix asphalt technology on asphalt physical and mechanical properties, Construct. Build. Mater. 112 (2016) 800–806.

[19] H. Hou, T. Wang, S. Wu, Y. Xue, R. Tan, J. Chen, M. Zhou, Investigation on the pavement performance of asphalt mixture based on predicted dynamic modulus, Construct. Build. Mater. 106 (2016) 11–17.

[20] Q. Dai, Prediction of dynamic modulus and phase angle of stone-based composites using a micromechanical finite-element approach, ASCE J. Mater. Civ. Eng. 22 (2010) 618–627.

[21] M.D. Nazzal, Md.T. Iqbal, S.S. Kim, A.R. Abbas, M. Akentuna, T. Quasem, Evaluation of the long-term performance and life cycle costs of GTR asphalt pavements, Construct. Build. Mater. 114 (2016) 261–268.

[22] P. Ayar, F.M. Navarro, M.C. Rubio-G, The healing capability of asphalt pavements: a state of the art review, J. Cleaner Product. 113 (2016) 28–40.

[23] L. Premkumar, W.R. Vavrik, Enhancing pavement performance prediction models for the Illinois Tollway System, Int. J. Pavement Res. Technol. 9 (2016) 14–19.

[24] Y.Y. Hong, J.Y. Hao, W.X. Cang, Pavement performance prediction methods and maintenance cost based on the structure load, Proc. Eng. 137 (2016) 41–48.

[25] P. Lowe, N. Ward, England's rural futures: a socio-geographical approach to scenarios analysis, Regional Studies 43 (10) (2009) 1319–1332.

[26] P.R. Kaufmann, Integrating factor analysis and the Delphi method in scenario development: A case study of Dalmatia, Croatia Appl. Geogr. 71 (2016) 56–68.

[27] S. Arnold, The Theory of Linear Models and Multivariate Analysis, John Wiley & Sons, New York, 1981.

[28] C.L. Hwang, K.S. Yoon, Multiple Attribute Decision Making, Springer Verlag, Berlin, 1981.

[29] R.A. Johnson, D.W. Wichern, Multivariate Statistical Analysis, 6th ed., Pearson Prentice Hall, Upper Saddle River,N.J, 2007.

[30] H.F. Kaiser, The varimax criterion for analytic rotation in factor analysis, Psychometrika 23 (3) (1958) 187–200.

[31] T.W. Anderson, H. Rubin, Statistical inference in factor analysis, in: Proceedings of the Third Berkeley Symposium on Mathematical Statistics and Probability, University of California Press, Berkeley and Los Angeles, 1956, pp. V111–150.

[32] JTG E20-2011, Standard Test Methods of Bitumen and Bituminous Mixtures for Highway Engineering.

[33] T. Kuennen, In-field Experience Revises Superpave Guidelines. Pavement Maintenance and Reconstruction (1998).

[34] H. Fu, L. Xie, D. Dou, Storage stability and compatibility of asphalt binder modified by SBS graft copolymer, Construct. Build. Mater. 21 (7) (2007) 1528–1533.

[35] Xu Hui-ning, Tan Yi-qiu, Li Xiao-ming, Tian Geng-liang. Research on Relationship Between Marshall Stability and Grading Curve Trait of Asphalt Mixture. Highway 08 (2008) 213-217.

[36] P. Yong, S. Lijun, S. Yongjiu, W. Yuanqing, Influence factors of shear resistance of asphalt mixture, J. Southeast University (Natural Science Edition) 2 (2007).

[37] R. Xiong, S. Chen, B. Guan, Application of grey entropy method to analyze influencing factors of durability of asphalt mixture under freeze-thaw and corrosion, J. Highway Transport. Res. Dev. 01 (2013) 28–32.

[38] Z. Fu, Z.G. Feng, Durability of asphalt mixture, J. Jilin Inst. Architect. Civil Eng. 03 (2010) 25–28.

[39] W. Chen, Research on Durability of Stone Matrix Asphalt, Chang'an University, 2009.

[40] H.H. Harman, Modern Factor Analysis, 3rd ed., University of Chicago Press, Chicago, 1976.

[41] L. Wang, L. Yang, Spline-Backfitted Kernel Smoothing of nonlinear additive auto regression model, Ann. Stat. 35 (2007) 2474–2503.

[42] J.Z. Huang, H. Shen, Functional coefficient regression models for nonlinear time series: a polynomial spline approach, Scared. J. Stat. 31 (2004) 515–534.